Phase-Sensitive Quantum Measurement without Controlled Operations

Yilun Yang, Arthur Christianen, Mari Carmen Bañuls, Dominik S. Wild, and J. Ignacio Cirac
Max-Planck-Institut für Quantenoptik, Hans-Kopfermann-Str. 1, D-85748 Garching, Germany
and Munich Center for Quantum Science and Technology (MCQST), Schellingstr. 4, D-80799 München, Germany

(Received 29 August 2023; revised 11 April 2024; accepted 3 May 2024; published 28 May 2024)

Many quantum algorithms rely on the measurement of complex quantum amplitudes. Standard approaches to obtain the phase information, such as the Hadamard test, give rise to large overheads due to the need for global controlled-unitary operations. We introduce a quantum algorithm based on complex analysis that overcomes this problem for amplitudes that are a continuous function of time. Our method only requires the implementation of real-time evolution and a shallow circuit that approximates a short imaginary-time evolution. We show that the method outperforms the Hadamard test in terms of circuit depth and that it is suitable for current noisy quantum computers when combined with a simple error-mitigation strategy.

DOI: 10.1103/PhysRevLett.132.220601

Introduction.—The complex phases of quantum amplitudes play an essential role in quantum algorithms [1–6] and quantum sensing [7]. Many algorithms require measuring the relative phase between two quantum states [8–17]. A common subroutine for this purpose is the Hadamard test, which converts phase information into probabilities by means of interference [18]. Despite impressive experimental progress, the Hadamard test remains out of reach for most applications owing to the challenge of implementing the required controlled-unitary operation. In this Letter, we propose an alternative method to determine the complex overlap between certain states that uses no ancillary qubits or global controlled-unitary operations. Unlike other ancilla-free schemes [12,19], our approach does not require the preparation of superpositions with a reference state, which are highly susceptible to noise [20–25]. Instead of interference, our method hinges on the principles of complex analysis.

The proposed approach applies to overlaps of the form of the (generalized) Loschmidt amplitude

$$\mathcal{G}(t) = \langle \psi' | e^{-iHt} | \psi \rangle, \tag{1}$$

where H is a local Hamiltonian. Our algorithm requires that $|\psi\rangle$ has a short correlation length and that $|\psi'\rangle$ can be prepared using a unitary circuit. These assumptions are needed to be able to efficiently apply a short imaginary-time evolution to $|\psi\rangle$ [26–34] and to perform a projective measurement onto the final state $|\psi'\rangle$ [35]. The absolute value $|\mathcal{G}(t)|$ can be obtained by repeatedly evolving $|\psi\rangle$ and averaging over projective measurements onto $|\psi'\rangle$. Here, we describe how to obtain the phase.

Equation (1) includes several cases of interest. When $|\psi'\rangle = |\psi\rangle$, $\mathcal{G}(t)$ is the Fourier transform of the local density of states, which has applications in the study of quantum chaos [36,37], in optimal measurements of multiple expectation values [14], and in estimating energy eigenvalues [9,10,13,15,17]. The case when $|\psi'\rangle = Ae^{-iHt'}|\psi\rangle$, for a local unitary A, is relevant for probing thermal properties of many-body systems [12,38–40].

The key idea underlying our method is to view $\mathcal{G}$ as a function of a complex variable z. Assuming that $\mathcal{G}(z)$ is analytic and nonzero, the Cauchy-Riemann equations imply that the real-time derivative of the phase of $\mathcal{G}(z)$ is equal to the derivative of $\ln|\mathcal{G}(z)|$ along the imaginary-time direction. We use this relation to obtain the desired phase by carrying out the following three steps on a quantum computer (see Fig. 1). First, a quantum circuit applies an evolution under the Hamiltonian H for a short *imaginary time* h to the initial state $|\psi\rangle$ [26–31]. Second, we evolve the system under H for the *real time* t. Third, we perform a projective measurement onto the state $|\psi'\rangle$ by inverting the circuit that prepares $|\psi'\rangle$ from a computational basis state, followed by measurements in the computational basis. Using these steps, we can estimate $|\mathcal{G}(t \pm ih)|$. This yields a finite-difference approximation to the imaginary-time derivative of $\ln|\mathcal{G}(z)|$, which is equal to the real-time derivative of the phase. We finally compute the phase of the Loschmidt amplitude by repeating these steps for different values of t and numerically integrating the derivative, starting from a time at which the phase is known.

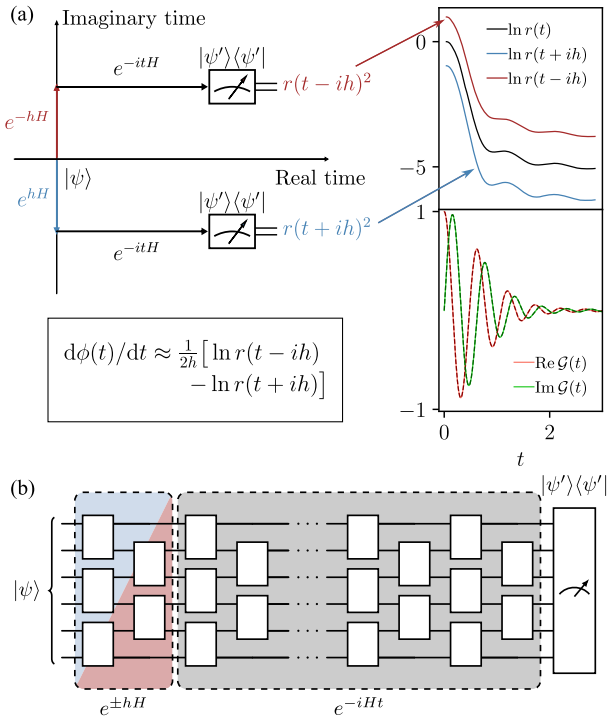

FIG. 1. (a) The time derivative of the complex phase $\phi(t)$ of Loschmidt amplitude $\mathcal{G}(t)$ can be estimated from $r(t \pm ih) = |\langle\psi'|e^{-iHt}e^{\pm hH}|\psi\rangle|$. The right panel shows the result of our approach with $h = 0.1$ for the transverse-field Ising chain, Eq. (8), of length $N = 40$. The solid lines on the lower right correspond to the complex Loschmidt amplitude obtained from the algorithm, while the overlapping dashed lines indicate the exact result. (b) Circuit to measure $r(t \pm ih)$. For initial product states, the rescaled imaginary-time evolution has the same brickwork layout as a single real-time Trotter step.

We show below that our method is efficient if $|\mathcal{G}(t \pm ih)|$ is bounded from below by an inverse polynomial in the system size N. For product states $|\psi'\rangle = |\psi\rangle$, however, the Loschmidt amplitude decays as a Gaussian function on a timescale $\mathcal{O}(1/\sqrt{N})$ [41]. In this case, our approach will be inefficient even for short constant times, for which the Loschmidt amplitude can be computed by a polynomial-time, classical algorithm [42]. By contrast, no efficient classical algorithm is known for the case $|\psi'\rangle = Ae^{-iHt'}|\psi\rangle$. Since the real- and imaginary-time evolution operators commute, our method can be used to compute the phase as a function of $t - t'$, with the expectation value $\langle\psi|e^{iHt'}Ae^{-iHt'}|\psi\rangle$ serving as the reference for the integration. This is expected to be classically hard even for small $t - t'$ since computing the reference value at times $t' = \mathrm{poly}(N)$ is BQP-complete [43].

Although our approach is based on the analytic properties of a function of a continuous variable, we show below that it also works well in the discrete setting of Trotter evolution. Hence, the method applies to both circuit-based quantum computers and to analog quantum simulators supplemented by shallow circuits to implement the imaginary-time evolution. To demonstrate the suitability of the method for near-term quantum devices, we combine it with a simple error-mitigation strategy [44–49] and show numerically that the phase can be reliably recovered in a system of $N = 24$ qubits. Beyond providing a viable alternative to the Hadamard test on near-term quantum computers, our method may be useful in the early fault-tolerant regime as the absence of controlled global operations significantly reduces the circuit depth.

Theoretical approach.—To formally describe the algorithm, we consider the complex variable $z = t - i\beta$, where t represents real time and β stands for imaginary time or inverse temperature. The generalized Loschmidt amplitude, Eq. (1), can be decomposed into its absolute value and phase according to

$$\mathcal{G}(z) = r(z)e^{i\phi(z)}, \tag{2}$$

where $0 \le r(z) \le 1$ and $\phi(z)$ is real. In a system of finite size, the Loschmidt amplitude can be written as a sum of exponentials by expanding the states $|\psi\rangle$ and $|\psi'\rangle$ in the energy eigenbasis. The logarithm $\ln \mathcal{G}(z)$ is therefore holomorphic everywhere except when $\mathcal{G}(z) = 0$. For an analytic branch of $\phi(z)$, the Cauchy-Riemann equations applied to $\ln \mathcal{G}(z) = \ln r(z) + i\phi(z)$ give

$$\frac{\partial}{\partial t}\phi(z) = \frac{\partial}{\partial \beta}[\ln r(z)]. \tag{3}$$

Therefore, if $\mathcal{G}(t) \neq 0$ in the interval $[t_1, t_2]$, the phase difference $\phi(t_2) - \phi(t_1)$ can be computed as

$$\phi(t_2) - \phi(t_1) = \int_{t_1}^{t_2} \frac{\partial}{\partial \beta}[\ln r(z)]_{|\beta=0}\mathrm{d}t. \tag{4}$$

If the phase $\phi(t_1)$ is known, then $\phi(t_2)$ may be computed from the partial derivative of $r(z)$ along the imaginary-time direction. In practice, we numerically approximate the partial derivative by the midpoint formula

$$\frac{\partial}{\partial \beta}[\ln r(z)]_{|\beta=0} \approx \frac{\ln r(t-ih) - \ln r(t+ih)}{2h}, \tag{5}$$

where h is a small parameter.

This procedure is well defined for $r(t \pm ih) > 0$ in the interval $[t_1, t_2]$. To bound the computational errors, we make the stronger assumption that $|\ln r(z)| \le cN$ at all points in the complex plane within distance a of the interval $[t_1, t_2]$, for constants c and $a > h$. In the case of Trotter evolution, we make analogous assumptions for closely related functions [50]. We highlight, however, that our approach can be extended to treat zeros in $\mathcal{G}(t)$ by separately considering the resulting discontinuities in the phase [50].

The above analysis has reduced the problem to measuring the absolute values $r(t \pm ih)^2$. It involves nonunitary imaginary-time evolution that cannot be directly applied. However, Motta *et al.* [27] showed that $e^{\pm hH}$ can be simulated by a unitary circuit for short times h if the spatial correlations of $|\psi\rangle$ decay exponentially with correlation length ξ and H is a local Hamiltonian. For each local term H_m in the Hamiltonian, it is possible to approximate $e^{\pm hH_m}|\psi\rangle \approx c_m^{\pm} V_m^{\pm}|\psi\rangle$, where $V_m^{\pm}$ is a local unitary and $c_m^{\pm} = \sqrt{\langle\psi|e^{\pm 2hH_m}|\psi\rangle}$ accounts for the normalization. Since h is small, the product over all $V_m^{\pm}/c_m^{\pm}$ (in arbitrary order) is a good approximation of e^{-hH}. The operators $V_m^{\pm}$ act on $\mathcal{O}[(\xi \log N)^d]$ qubits in d spatial dimensions and the complexity of computing $V_m^{\pm}$ is quasipolynomial in N for $d > 1$. This renders the approach challenging for large ξ. Below, we focus on the simplest case of product states, for which the unitaries $V_m^{\pm}$ act on the same sites as H_m and can be efficiently computed. The resulting circuit has the same structure as a single Trotter step [50].

Error analysis.—We next analyze the error in the estimated phase arising from the different approximations in our algorithm. The approximation error of the imaginary-time evolution is dominated by the first-order Trotter decomposition, which results in the phase error [50]

$$\Delta\phi_{\mathrm{ITE}} = \mathcal{O}(Nth^2). \tag{6}$$

The factor $t = t_2 - t_1$ accounts for the accumulation of errors in the integral in Eq. (4). While the real-time evolution can be carried out exactly on analog quantum simulators, digital quantum computers incur an additional Trotter error, leading to the phase error [50]

$$\Delta\phi_{\mathrm{RTE}} = \mathcal{O}(Nt^2\tau^p). \tag{7}$$

Here, τ is the time of a single Trotter step, p is the order of the Trotter decomposition [59], and we again included the accumulation of errors in Eq. (4). Numerical differentiation and integration give rise to additional errors. They can, however, be safely ignored for practical orders of the Trotter expansion ($p \leq 4$) as they are asymptotically at most as big as $\Delta\phi_{\mathrm{ITE}}$ and $\Delta\phi_{\mathrm{RTE}}$ [50].

We verify these analytic estimates using numerical results for the transverse-field Ising chain, whose Hamiltonian is given by

$$H = -J\sum_{i=1}^{N-1} S_i^z S_{i+1}^z + g\sum_{i=1}^{N} S_i^x. \tag{8}$$

Throughout this work, we set $J = 1$ and $g = 0.5$, corresponding to the ferromagnetic phase. Both states $|\psi\rangle$ and $|\psi'\rangle$ are chosen as $|\uparrow\uparrow\uparrow\cdots\rangle$. For the Trotter decomposition, we alternate between the ferromagnetic and transverse-field terms.

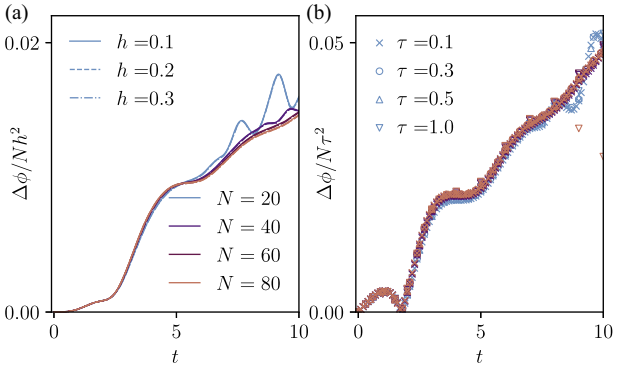

FIG. 2. Error in the phase of Loschmidt amplitude, $\Delta\phi$, computed using our approach for the transverse-field Ising chain, Eq. (8). (a) $\Delta\phi/Nh^2$ as a function of time t with fixed real-time Trotter step $\tau = 0.01$ for different values of the imaginary-time step h and different system sizes N. (b) $\Delta\phi/N\tau^2$ for $h = 0.01$ and different values of τ and N. The color coding is the same as in (a).

Figure 2 shows the error in the phase computed using our approach. The numerical results were obtained by matrix product state simulations with bond dimension 200, for which truncation errors are negligible [50]. In Fig. 2(a), we set $\tau = 0.01$ such that the error in the imaginary-time evolution dominates. The phase error collapses onto a single curve upon dividing by Nh^2, which confirms the predicted error due to imaginary-time evolution, Eq. (6). Similarly, we set $h = 0.01$ in Fig. 2(b) to isolate the effect of the real-time Trotter error. The collapse of the data agrees with Eq. (7).

In addition to numerical errors, any experiment incurs statistical errors. Given M measurements, a probability p estimated by counting successful outcomes will have a multiplicative error $\sqrt{(1-p)/Mp}$, governed by the standard deviation of the binomial distribution. According to Eq. (5), for the measured probabilities $p_{\pm}(t) = r(t \pm ih)^2/\prod_m (c_m^{\pm})^2$, this contributes an additive error

$$\Delta\phi_{\mathrm{S}} = \mathcal{O}\left(\frac{It}{h\sqrt{M}}\right) \tag{9}$$

to the final phase for M measurements per time step. The integral in Eq. (4) is included in the factor $I = \int_{t_1}^{t_2} \mathrm{d}t' \left[\sqrt{1/p_+(t')} + \sqrt{1/p_-(t')}\right]/t$. In contrast to the previous errors, the statistical error depends on the magnitude of the measured probabilities.

Comparison with existing methods.—To compare our approach to existing methods, we consider the error $\Delta\mathcal{G}$ in the complex Loschmidt amplitude $\mathcal{G}$. This error is related to the phase error, $\Delta\phi$, by $|\Delta\mathcal{G}|^2 = \Delta r^2 + (r\Delta\phi)^2$. Here, Δr is the error from an independent measurement of r, which only requires the Trotterized circuit without imaginary-time evolution. To bound Δr by ϵ, we need a circuit of depth $D_r = \mathcal{O}(t/\tau) = \mathcal{O}(t^{1+(1/p)}N^{(1/p)}/\epsilon^{(1/p)})$ and a number of

TABLE I. Circuit depth D and number of measurements M to estimate the complex Loschmidt amplitude $\mathcal{G}$ with additive error ϵ. All protocols use a real-time Trotter decomposition of order p. The Hadamard test is implemented using a single ancilla qubit with swap operations in d spatial dimensions. The latter two methods require M measurements at each intermediate state or time step, but the corresponding values of the phase are also returned. For these approaches, we only consider initial product states and ϵ bounds the error $r\Delta\phi$ arising from the uncertainty in the phase. The quantities $\tilde{I}$ and I depend on the intermediate amplitudes in these sequences; see text and Supplemental Material [50].

Method	D	M
Hadamard test	$\mathcal{O}(t^{1+(1/p)}N^{1+(1/d)+(1/p)}/\epsilon^{(1/p)})$	$\mathcal{O}(1/\epsilon^2)$
Sequential interferometry	$\mathcal{O}(r^{(1/p)}t^{1+(1/p)}N^{(2/p)}/\epsilon^{(1/p)})$	$\mathcal{O}(\tilde{I}^2r^2N^2/\epsilon^2)$
This work	$\mathcal{O}(r^{(1/p)}t^{1+(2/p)}N^{(1/p)}/\epsilon^{(1/p)})$	$\mathcal{O}(I^2r^3t^3N/\epsilon^3)$

$M_r = \mathcal{O}(1/\epsilon^2)$ measurements [50]. For the term $r\Delta\phi$, we bound the individual contributions to the phase error. For instance, $r\Delta\phi_{\mathrm{ITE}} < \epsilon$ implies that $h = \mathcal{O}(\sqrt{\epsilon/rNt})$. A similar bound on the real-time evolution gives $\tau = \mathcal{O}[(\epsilon/rNt^2)^{(1/p)}]$, resulting in the circuit depth $D = \mathcal{O}(r^{(1/p)}t^{1+(2/p)}N^{(1/p)}/\epsilon^{(1/p)})$. Bounding the statistical error yields the number of measurements $M = \mathcal{O}(I^2r^3t^3N/\epsilon^3)$ for each time step. We note that when r is bounded from below by a constant, the cost of estimating ϕ dominates.

We compare this resource cost to the Hadamard test and sequential interferometry [12]. The latter method employs a reference state whose Loschmidt amplitude, including the phase, is known. The details of these two methods are described in the Supplemental Material [50]. Table I summarizes the resource cost for each method. For a constant evolution time t, the circuit depth needed for our algorithm is reduced by a factor $\mathcal{O}(N^{1+1/d})$ compared to the Hadamard test with swaps, and by $\mathcal{O}(N^{1/p})$ compared to sequential interferometry. This improvement is particularly significant for noisy quantum computers, for which circuit depth is the key limiting factor.

Applications.—For practical applications of our protocol, it is important to consider the role of noise. We propose a simple rescaling strategy based on previous work to mitigate the effects of noise [49]. The key observation is that errors are unlikely to drive the system toward the target state $|\psi'\rangle$. Hence, the measured probabilities are decreased in a consistent fashion, which can be mitigated by rescaling with the probability of having no noise. This is equivalent to zero-noise extrapolation with an exponential fitting function [44,60,61]. Below, we simply use the known noise rate for rescaling. In practice, the rescaling factor can be determined by enhancing the noise or by measuring the survival probability after forward plus backward evolution [49].

As a proof of concept, we apply our approach to compute the local density of states (LDOS) $d(E)$ through the Fourier transform

$$d(E) = \langle\psi|\delta(E-H)|\psi\rangle = \frac{1}{2\pi}\int_{-\infty}^{\infty}\mathcal{G}(t)e^{iEt}\mathrm{d}t. \tag{10}$$

If the initial state has a sufficiently large overlap with the ground state, its LDOS enables determining the ground state energy. In quantum chemistry, this can hold even for product states, rendering our approach particularly suitable [62]. We further note that our approach is compatible with

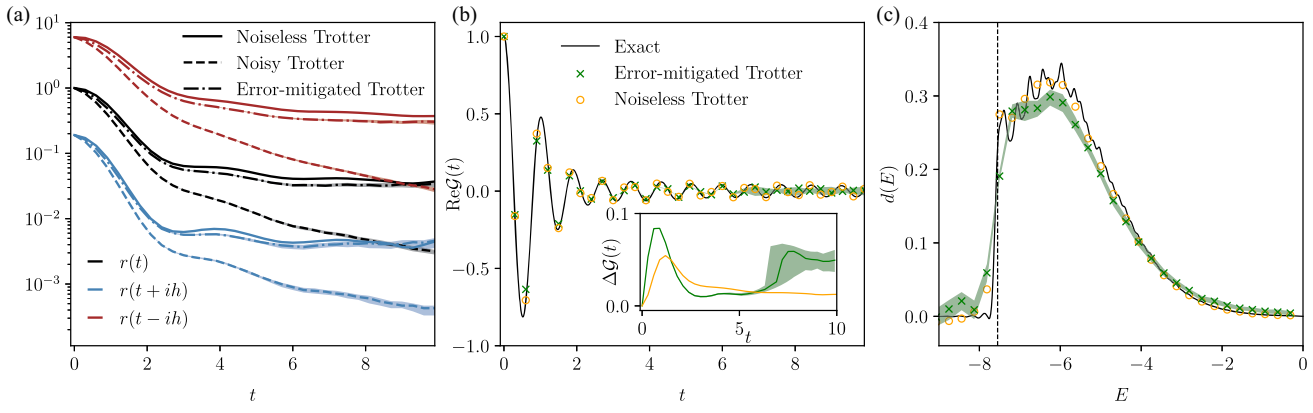

FIG. 3. (a) Absolute value of the Loschmidt amplitudes for an Ising chain of length $N = 24$ with initial state $|\uparrow\uparrow\uparrow\cdots\rangle$ and Trotter step sizes $\tau = h = 0.3$. The dashed lines include single-qubit depolarizing noise with probability $\gamma = 3\times10^{-3}$ after each gate. The dash-dotted lines are obtained by the error mitigation described in the text. We quantify the statistical error of the error-mitigated curves by simulating 100 experiments, each of which uses $M = 10^6$ measurements to estimate the survival probability. The dash-dotted line corresponds to the median of the 100 experiments, while the shaded areas indicate the range between the first and third quartile. (b) Real part of the Loschmidt amplitude computed from the data in (a) using our algorithm. The exact value under continuous time evolution is plotted for reference. The inset shows the absolute difference of the reconstructed values from the exact amplitude. (c) The LDOS obtained through discrete Fourier transform from the data in (b). The vertical, dashed line indicates the exact ground state energy $E_0 \approx -7.55$.

recent proposals that classically process the Loschmidt amplitudes at different times in order to solve the general quantum eigenvalue estimation problem [10,50] with Heisenberg-limited scaling [13,15,17].

We apply our approach to compute the LDOS of $|\psi\rangle = |\uparrow\uparrow\uparrow\cdots\rangle$ in an Ising chain of system size $N = 24$. We numerically carry out the Trotter evolution with Trotter steps $\tau = h = 0.3$ using the Cirq library [63]. We add single-qubit depolarizing noise of rate $\gamma = 3 \times 10^{-3}$ after each layer of the quantum circuit. We average over 5000 trajectories of a Monte Carlo wave function simulation to obtain the probabilities $p_{\pm}$. The results are shown in Fig. 3. Here, we have included statistical noise by simulating the experimental sampling procedure (see caption).

Figure 3(a) shows that the depolarizing noise is mitigated well by rescaling $r^2(t)$ and $r^2(t \pm ih)$ by $(1-\gamma)^{ND}$. The error in the reconstructed Loschmidt amplitude remains small within the range of t in Fig. 3(b). We estimate the LDOS of the initial state by a discrete Fourier transform of the data in Fig. 3(b) and similar data for the imaginary part of $\mathcal{G}(t)$. The energy resolution is $\pi/t_{\max} \approx 0.31$, determined by the maximum time $t_{\max} = 10$. We show the result in Fig. 3(c) for both noisy, error-mitigated (green) and noiseless (orange) Trotter simulations. For reference, we also include the exact result (black line), which is broadened by a Gaussian of width 0.08. For both Trotter simulations, the first point with $d(E) > 0.1$ appears at $E \approx -7.50$, while the exact ground state energy is $E_0 \approx -7.55$.

Summary and outlook.—We propose a quantum algorithm to estimate the phase of Loschmidt amplitudes applicable to states with short-ranged correlations. It can replace and outperform the Hadamard test for amplitudes that arise from continuous time evolution under a local Hamiltonian. While our analysis focused on generalized Loschmidt amplitudes, the approach can be readily extended to multiple time-evolution operators [50], which renders it applicable to many quantities of physical interest including transport coefficients [64–66] and out-of-time-ordered correlators [67,68]. The algorithm requires no ancillary qubits or controlled operations. When combined with a simple error-mitigation strategy, our algorithm may enable phase-sensitive measurements on current noisy quantum devices for system sizes that out of reach for other methods.

We thank Sandra Coll-Vinent, Sirui Lu, and Thomas O'Brien for insightful discussions about the sequential interferometry method, and Henrik Dreyer, Khaldoon Ghanem, Kévin Hémery, and Daniel Malz for valuable suggestions on applications of this algorithm. We acknowledge the support from the German Federal Ministry of Education and Research (BMBF) through FermiQP (Grant No. 13N15890) and EQUAHUMO (Grant No. 13N16066) within the funding program quantum technologies—from basic research to market. This research is part of the Munich Quantum Valley (MQV), which is supported by the Bavarian state government with funds from the Hightech Agenda Bayern Plus. D. S. W. has received funding from the European Union's Horizon 2020 research and innovation programme under the Marie Skłodowska-Curie Grant Agreement No. 101023276. The work was partially supported by the Deutsche Forschungsgemeinschaft (DFG, German Research Foundation) under Germany's Excellence Strategy—EXC-2111–390814868.

[1] P. Shor, Algorithms for quantum computation: Discrete logarithms and factoring, in *Proceedings of the 35th Annual Symposium on Foundations of Computer Science* (1994), pp. 124–134.
[2] A. Y. Kitaev, Quantum measurements and the abelian stabilizer problem, arXiv:quant-ph/9511026.
[3] E. Knill, G. Ortiz, and R. D. Somma, Optimal quantum measurements of expectation values of observables, Phys. Rev. A **75**, 012328 (2007).
[4] A. W. Harrow, A. Hassidim, and S. Lloyd, Quantum algorithm for linear systems of equations, Phys. Rev. Lett. **103**, 150502 (2009).
[5] N. Wiebe and C. Granade, Efficient Bayesian phase estimation, Phys. Rev. Lett. **117**, 010503 (2016).
[6] L. Clinton, J. Bausch, J. Klassen, and T. Cubitt, Phase estimation of local Hamiltonians on NISQ hardware, arXiv:2110.13584.
[7] C. L. Degen, F. Reinhard, and P. Cappellaro, Quantum sensing, Rev. Mod. Phys. **89**, 035002 (2017).
[8] D. Aharonov, V. Jones, and Z. Landau, *A polynomial quantum algorithm for approximating the jones polynomial* (Association for Computing Machinery, New York, NY, USA, 2006), pp. 427–436.
[9] T. E. O'Brien, B. Tarasinski, and B. M. Terhal, Quantum phase estimation of multiple eigenvalues for small-scale (noisy) experiments, New J. Phys. **21**, 023022 (2019).
[10] R. D. Somma, Quantum eigenvalue estimation via time series analysis, New J. Phys. **21**, 123025 (2019).
[11] S. McArdle, S. Endo, A. Aspuru-Guzik, S. C. Benjamin, and X. Yuan, Quantum computational chemistry, Rev. Mod. Phys. **92**, 015003 (2020).
[12] S. Lu, M. C. Bañuls, and J. I. Cirac, Algorithms for quantum simulation at finite energies, PRX Quantum **2**, 020321 (2021).
[13] L. Lin and Y. Tong, Heisenberg-limited ground-state energy estimation for early fault-tolerant quantum computers, PRX Quantum **3**, 010318 (2022).
[14] W. J. Huggins, K. Wan, J. McClean, T. E. O'Brien, N. Wiebe, and R. Babbush, Nearly optimal quantum algorithm for estimating multiple expectation values, Phys. Rev. Lett. **129**, 240501 (2022).
[15] Z. Ding and L. Lin, Even shorter quantum circuit for phase estimation on early fault-tolerant quantum computers with applications to ground-state energy estimation, PRX Quantum **4**, 020331 (2023).
[16] T. L. Patti, J. Kossaifi, A. Anandkumar, and S. F. Yelin, Quantum Goemans-Williamson algorithm with the

Hadamard test and approximate amplitude constraints, Quantum **7**, 1057 (2023).
[17] H. Ni, H. Li, and L. Ying, On low-depth algorithms for quantum phase estimation, Quantum **7**, 1165 (2023).
[18] R. Cleve, A. Ekert, C. Macchiavello, and M. Mosca, Quantum algorithms revisited, Proc. R. Soc. A **454**, 339 (1998).
[19] A. E. Russo, K. M. Rudinger, B. C. A. Morrison, and A. D. Baczewski, Evaluating energy differences on a quantum computer with robust phase estimation, Phys. Rev. Lett. **126**, 210501 (2021).
[20] R. Laflamme, E. Knill, W. H. Zurek, P. Catasti, and S. V. S. Mariappan, NMR Greenberger–Horne–Zeilinger states, Phil. Trans. R. Soc. A **356**, 1941 (1998).
[21] D. Leibfried, E. Knill, S. Seidelin, J. Britton, R. B. Blakestad, J. Chiaverini, D. B. Hume, W. M. Itano, J. D. Jost, C. Langer, R. Ozeri, R. Reichle, and D. J. Wineland, Creation of a six-atom 'Schrödinger cat' state, Nature (London) **438**, 639 (2005).
[22] C. Song, K. Xu, W. Liu, C.-P. Yang, S.-B. Zheng, H. Deng, Q. Xie, K. Huang, Q. Guo, L. Zhang, P. Zhang, D. Xu, D. Zheng, X. Zhu, H. Wang, Y.-A. Chen, C.-Y. Lu, S. Han, and J.-W. Pan, 10-qubit entanglement and parallel logic operations with a superconducting circuit, Phys. Rev. Lett. **119**, 180511 (2017).
[23] A. Omran, H. Levine, A. Keesling, G. Semeghini, T. T. Wang, S. Ebadi, H. Bernien, A. S. Zibrov, H. Pichler, S. Choi, J. Cui, M. Rossignolo, P. Rembold, S. Montangero, T. Calarco, M. Endres, M. Greiner, V. Vuletić, and M. D. Lukin, Generation and manipulation of Schrödinger cat states in Rydberg atom arrays, Science **365**, 570 (2019).
[24] K. X. Wei, I. Lauer, S. Srinivasan, N. Sundaresan, D. T. McClure, D. Toyli, D. C. McKay, J. M. Gambetta, and S. Sheldon, Verifying multipartite entangled Greenberger-Horne-Zeilinger states via multiple quantum coherences, Phys. Rev. A **101**, 032343 (2020).
[25] L. Bin, Y. Zhang, Q. P. Su, and C. P. Yang, Efficient scheme for preparing hybrid GHZ entangled states with multiple types of photonic qubits in circuit QED, Eur. Phys. J. Plus **137**, 1046 (2022).
[26] T. Jones, S. Endo, S. McArdle, X. Yuan, and S. C. Benjamin, Variational quantum algorithms for discovering Hamiltonian spectra, Phys. Rev. A **99**, 062304 (2019).
[27] M. Motta, C. Sun, A. T. K. Tan, M. J. O'Rourke, E. Ye, A. J. Minnich, F. G. S. L. Brandão, and G. K.-L. Chan, Determining eigenstates and thermal states on a quantum computer using quantum imaginary time evolution, Nat. Phys. **16**, 205 (2020).
[28] S.-H. Lin, R. Dilip, A. G. Green, A. Smith, and F. Pollmann, Real- and imaginary-time evolution with compressed quantum circuits, PRX Quantum **2**, 010342 (2021).
[29] H. Nishi, T. Kosugi, and Y.-i. Matsushita, Implementation of quantum imaginary-time evolution method on NISQ devices by introducing nonlocal approximation, npj Quantum Inf. **7**, 85 (2021).
[30] P. Jouzdani, C. W. Johnson, E. R. Mucciolo, and I. Stetcu, Alternative approach to quantum imaginary time evolution, Phys. Rev. A **106**, 062435 (2022).
[31] H. Kamakari, S.-N. Sun, M. Motta, and A. J. Minnich, Digital quantum simulation of open quantum systems using quantum imaginary–time evolution, PRX Quantum **3**, 010320 (2022).
[32] A. Gilyén, Y. Su, G. H. Low, and N. Wiebe, Quantum singular value transformation and beyond: Exponential improvements for quantum matrix arithmetics, in *Proceedings of the 51st Annual ACM SIGACT Symposium on Theory of Computing, STOC 2019* (Association for Computing Machinery, New York, NY, USA, 2019), pp. 193–204.
[33] Z. Holmes, G. Muraleedharan, R. D. Somma, Y. Subasi, and B. Şahinoğlu, Quantum algorithms from fluctuation theorems: Thermal-state preparation, Quantum **6**, 825 (2022).
[34] D. An, J.-P. Liu, and L. Lin, Linear combination of Hamiltonian simulation for nonunitary dynamics with optimal state preparation cost, Phys. Rev. Lett. **131**, 150603 (2023).
[35] The measurement is defined by a complete, mutually orthogonal set of projection operators that includes $|\psi'\rangle\langle\psi'|$. We assign 1 to an outcome of $|\psi'\rangle$ and 0 all other outcomes. For any state that can be efficiently prepared from a product state in the computational basis using unitary circuits, one can invert the preparation circuit and perform local measurements in the computational basis to realize the projective measurement. Such states include time evolved product states and injective matrix product states [69].
[36] G. Benenti and G. Casati, Quantum-classical correspondence in perturbed chaotic systems, Phys. Rev. E **65**, 066205 (2002).
[37] M. F. Andersen, A. Kaplan, T. Grünzweig, and N. Davidson, Decay of quantum correlations in atom optics billiards with chaotic and mixed dynamics, Phys. Rev. Lett. **97**, 104102 (2006).
[38] A. Schuckert, A. Bohrdt, E. Crane, and M. Knap, Probing finite-temperature observables in quantum simulators of spin systems with short-time dynamics, Phys. Rev. B **107**, L140410 (2023).
[39] K. Hémery, K. Ghanem, E. Crane, S. L. Campbell, J. M. Dreiling, C. Figgatt, C. Foltz, J. P. Gaebler, J. Johansen, M. Mills, S. A. Moses, J. M. Pino, A. Ransford, M. Rowe, P. Siegfried, R. P. Stutz, H. Dreyer, A. Schuckert, and R. Nigmatullin, Measuring the Loschmidt amplitude for finite-energy properties of the Fermi-Hubbard model on an ion-trap quantum computer, arXiv:2309.10552.
[40] K. Ghanem, A. Schuckert, and H. Dreyer, Robust extraction of thermal observables from state sampling and real-time dynamics on quantum computers, Quantum **7**, 1163 (2023).
[41] M. Hartmann, G. Mahler, and O. Hess, Gaussian quantum fluctuations in interacting many particle systems, Lett. Math. Phys. **68**, 103 (2004).
[42] D. S. Wild and A. M. Alhambra, Classical simulation of short-time quantum dynamics, PRX Quantum **4**, 020340 (2023).
[43] D. Janzing and P. Wocjan, Ergodic quantum computing, Quantum Inf. Process. **4**, 129 (2005).
[44] K. Temme, S. Bravyi, and J. M. Gambetta, Error mitigation for short-depth quantum circuits, Phys. Rev. Lett. **119**, 180509 (2017).

[45] S. Endo, S. C. Benjamin, and Y. Li, Practical quantum error mitigation for near-future applications, Phys. Rev. X **8**, 031027 (2018).
[46] A. Kandala, K. Temme, A. D. Córcoles, A. Mezzacapo, J. M. Chow, and J. M. Gambetta, Error mitigation extends the computational reach of a noisy quantum processor, Nature (London) **567**, 491 (2019).
[47] T. E. O'Brien, S. Polla, N. C. Rubin, W. J. Huggins, S. McArdle, S. Boixo, J. R. McClean, and R. Babbush, Error mitigation via verified phase estimation, PRX Quantum **2**, 020317 (2021).
[48] Z. Cai, R. Babbush, S. C. Benjamin, S. Endo, W. J. Huggins, Y. Li, J. R. McClean, and T. E. O'Brien, Quantum error mitigation, arXiv:2210.00921.
[49] Y. Yang, A. Christianen, S. Coll-Vinent, V. Smelyanskiy, M. C. Bañuls, T. E. O'Brien, D. S. Wild, and J. I. Cirac, Simulating prethermalization using near-term quantum computers, PRX Quantum **4**, 030320 (2023).
[50] See Supplemental Material at http://link.aps.org/supplemental/10.1103/PhysRevLett.132.220601, which includes Refs. [51–58], for a detailed analysis of errors, for resource cost estimates, for extensions of the algorithm to treat zeros in the Loschmidt amplitude and to multiple time-evolution operators, for applications of the algorithm, and for details on numerical simulations.
[51] A. Quarteroni, R. Sacco, and F. Saleri, *Numerical Mathematics* (Springer, Berlin, Heidelberg, 2006).
[52] H. Touchette, The large deviation approach to statistical mechanics, Phys. Rep. **478**, 1 (2009).
[53] T. Monz, P. Schindler, J. T. Barreiro, M. Chwalla, D. Nigg, W. A. Coish, M. Harlander, W. Hänsel, M. Hennrich, and R. Blatt, 14-qubit entanglement: Creation and coherence, Phys. Rev. Lett. **106**, 130506 (2011).
[54] A. Gambassi and A. Silva, Large deviations and universality in quantum quenches, Phys. Rev. Lett. **109**, 250602 (2012).
[55] M. Heyl, A. Polkovnikov, and S. Kehrein, Dynamical quantum phase transitions in the transverse-field Ising model, Phys. Rev. Lett. **110**, 135704 (2013).
[56] N. Friis, O. Marty, C. Maier, C. Hempel, M. Holzäpfel, P. Jurcevic, M. B. Plenio, M. Huber, C. Roos, R. Blatt, and B. Lanyon, Observation of entangled states of a fully controlled 20-qubit system, Phys. Rev. X **8**, 021012 (2018).
[57] A. Ozaeta and P. L. McMahon, Decoherence of up to 8-qubit entangled states in a 16-qubit superconducting quantum processor, Quantum Sci. Technol. **4**, 025015 (2019).
[58] A. W. Harrow, S. Mehraban, and M. Soleimanifar, Classical algorithms, correlation decay, and complex zeros of partition functions of quantum many-body systems, in *Proceedings of the 52nd Annual ACM SIGACT Symposium on Theory of Computing, STOC 2020* (Association for Computing Machinery, New York, NY, USA, 2020), pp. 378–386.
[59] A. M. Childs, Y. Su, M. C. Tran, N. Wiebe, and S. Zhu, Theory of trotter error with commutator scaling, Phys. Rev. X **11**, 011020 (2021).
[60] Y. Li and S. C. Benjamin, Efficient variational quantum simulator incorporating active error minimization, Phys. Rev. X **7**, 021050 (2017).
[61] Y. Kim, A. Eddins, S. Anand, K. X. Wei, E. van den Berg, S. Rosenblatt, H. Nayfeh, Y. Wu, M. Zaletel, K. Temme, and A. Kandala, Evidence for the utility of quantum computing before fault tolerance, Nature (London) **618**, 500 (2023).
[62] B. Bauer, S. Bravyi, M. Motta, and G. K.-L. Chan, Quantum algorithms for quantum chemistry and quantum materials science, Chem. Rev. **120**, 12685 (2020).
[63] Cirq Developers, Cirq (2022), 10.5281/zenodo.10247207.
[64] K. Agarwal, S. Gopalakrishnan, M. Knap, M. Müller, and E. Demler, Anomalous diffusion and griffiths effects near the many-body localization transition, Phys. Rev. Lett. **114**, 160401 (2015).
[65] M. Kanász-Nagy, I. Lovas, F. Grusdt, D. Greif, M. Greiner, and E. A. Demler, Quantum correlations at infinite temperature: The dynamical Nagaoka effect, Phys. Rev. B **96**, 014303 (2017).
[66] D. E. Parker, X. Cao, A. Avdoshkin, T. Scaffidi, and E. Altman, A universal operator growth hypothesis, Phys. Rev. X **9**, 041017 (2019).
[67] K. Hashimoto, K. Murata, and R. Yoshii, Out-of-time-order correlators in quantum mechanics, J. High Energy Phys. 10 (2017) 138.
[68] M. Sajjan, V. Singh, R. Selvarajan, and S. Kais, Imaginary components of out-of-time-order correlator and information scrambling for navigating the learning landscape of a quantum machine learning model, Phys. Rev. Res. **5**, 013146 (2023).
[69] D. Malz, G. Styliaris, Z.-Y. Wei, and J. I. Cirac, Preparation of matrix product states with log-depth quantum circuits, arXiv:2307.01696.